A major purpose of the Technical Information Center is to provide the broadest dissemination possible of information contained in DOE's Research and Development Reports to business, industry, the academic community, and federal, state and local governments.

Although a small portion of this report is not reproducible, it is being made available to expedite the availability of information on the research discussed herein.

1

LA-UR -89-2138

TITLE   PROTOTYPE TESTING FOR A HYBRID GAS-GUN/RAILGUN DEVICE

LA-UR--89-2138

DE89 014294

AUTHOR(S)   Jerald V. Parker

DISCLAIMER

Los Alamos
Los Alamos National Laboratory
Los Alamos, New Mexico 87545

PROTOTYPE TESTING FOR A HYBRID GAS-GUN/RAILGUN DEVICE

Jerald V. Parker

Los Alamos National Laboratory
Los Alamos, New Mexico 87545

INTRODUCTION

In 1984 Los Alamos began the design of the lethality test system (LTS), a facility to be used for the study of impact physics at velocities up to 15 km/s. The key component of LTS was an electromagnetic launcher capable of accelerating a 30 gram mass to 15 km/s [1]. By the time of the Preliminary Design Review (July 1985) it was known from laboratory experiments [2] that a conventional railgun was incapable of reaching 15 km/s starting at low velocity (~ 1 km/s) and a hybrid design was adopted for the LTS launcher. The hybrid launcher consisted of a two-stage hydrogen gun that preaccelerated the test mass to 6.5 km/s and an electromagnetic launcher for the final acceleration from 6.5 to 15 km/s. Design calculations predicted that injection into the railgun at 6.5 km/s would reduce ablation sufficiently to permit operation at 12 km/s with reasonable probability of achieving 15 km/s.

The hybrid launcher design adopted for LTS presents some unique mechanical and electrical issues. In particular, the hybrid design requires that the plasma armature be established in a high pressure gas environment behind the projectile. To address this issue, as well as to evaluate the mechanical and electrical design, a 1.83 meter long prototype of the electromagnetic launcher barrel was built and tested. This paper describes the prototype launcher tests and the performance achieved. In addition, testing of a plasma initiator operating in a high pressure gas environment is discussed.

The LTS development project was canceled in November, 1987, prior to operation of the full scale hybrid railgun so the feasibility of this approach was not established. The hybrid gas-gun/railgun concept is still being investigated at a small scale in a program at Sandia National Laboratory [3].

PROTOTYPE RAILGUN DESIGN

The prototype LTS railgun has the same cross-sectional configuration, shown in Figure 1, as the full-scale launcher. It differs only in length, being 1.83 meters long as compared to 22 meters for the LTS barrel. To achieve 15 km/s in a reasonable length, the LTS railgun design operates at high

pressure (3.2×10^8 Pa/45,000 PSI). Plasma leakage into joints in the rail-insulator structure is prevented by precompressing the structure using massive steel anvils bolted together on both sides with 57 mm diameter bolts spaced 114 mm center to center. The response of this railgun structure was analyzed in detail using a 2-D FEM code [4]. Prototype testing included measurement of rail motion to verify these design calculations.

The design bore diameter is 23.8 mm. The bore surface can be refinished by reaming in increments of 0.25 mm to a maximum of 26.2 mm. The rails are fabricated from ETP copper and the insulator facing the bore is Lexan polycarbonate backed by G-10 fiberglass-epoxy laminate. The calculated inductance gradient, including the effects of the steel structure, is 0.29 μH/m.

Three versions of this prototype were built and tested. The first version, designated LTS-P, utilized G-10 laminate for the insulating structural pieces as shown in Figure 1. The second version, designated LTS-HPP, was a high pressure version that utilized a commercial high impact strength ceramic (KYON® from Kennametal) in place of the G-10 laminate. The high modules of the ceramic was intended to reduce motion of the bore components during high current operation. The third version, designated LTS-IP, was identical to LTS-P except that it incorporated a plasma initiator (described below) and the rails incorporated a mechanical joint design that was needed for the full length barrel.

Figure 2 shows a side view of the prototype including the injector, muzzle vacuum chamber and external velocity measuring station. The two stage hydrogen gun was not available during prototype testing so all tests were performed with low velocity (~ 1 km/s) injection. The injector used commercial shotgun powder initiated with an electrically fired squib. A powder charge of 5.75 grams provided a consistent velocity of 1.05 km/s with the standard 8.9 gram projectile used during testing. The railgun bore was filled with a low pressure of air (25-50 Torr) on all tests to prevent electrical breakdown ahead of the projectile.

The power source for testing was a modular capacitor bank consisting of 7 modules, each with a capacitance of 1.36 mF and a series inductor of 11 μH. Turn on and crowbar switching used size D mercury ignitrons. All control and triggering is done using fiber optics to reduce electrical noise. The modules can be triggered independently to shape the current waveform.

DIAGNOSTICS

The principal electrical diagnostics are magnetic loops, oriented to measure the field from the rail current, and voltage measurements at breech and muzzle. The rail current probes are 5 mm x 8 mm loops wound with 50 turns of 0.18 mm diameter insulated copper wire. The probe coils are mounted 59 mm from the axis and provide a spatial resolution of the current distribution

of about 90 mm. The location of the rail current probes is shown in Figure 2. The probes for the HPP test could only be inserted between blocks of the KYON[9] ceramic so the number of probes and their position differs.

Breech and muzzle voltage were measured by connecting a 1000 ohm resistor across the rails and measuring the current in the resistor with a Pearson Electronics Model 411 current transformer. Projectile position was sensed at the entrance to the railgun by two high speed ($\sim$ 3 μs) pressure switches that respond to the injector gas pressure ($\sim$ 7x10^6 Pa) behind the projectile.

Measurement of rail displacement was accomplished with a commercial fiber optic motion sensor manufactured by Fotonics, Inc. The fiber assembly was mounted to the steel anvils with the probe tip projecting into the structure as shown in Figure 1. The back surface motion of the rail is measured with respect to the surface of the steel anvil. The resolution of this system is 8 μm over a linear range of $\pm$ 2 mm. The time response is determined by the photodetector and was less than 10 μs for these tests.

During most of the tests, a d.c. voltage of $\sim$ 200-500 V was applied to the rails by a battery power supply. Changes in the rail voltage were used to detect fuse contact with the rails and to measure the properties of the initiator plasma.

Projectile velocity was measured externally by a two-station break-wire located 1.5 m from the railgun. Each break-wire consisted of an 0.025 mm diameter tungsten wire mounted in a zigzag configuration over a 15 cm diameter plastic frame. Time resolution of the break signal was less than 0.5 μs resulting in a velocity accuracy of $\sim$ 1% up to 3.5 km/s. Above 3.5 km/s the signal is disturbed by ionized gas in the projectile bow shock and the measurement accuracy is reduced.

TEST RESULTS

Each configuration of the LTS prototype was tested over a range of currents from 200 kA to 1 MA. A summary of all the tests is presented in Table I. The significance of the entries in Table I can be appreciated by examining one of the tests (HPP-3) in more detail. The current waveform for test HPP-3 is shown in Figure 3. To reduce rail damage during fuse vaporization and plasma armature formation, only one power supply module is employed for the first 50 μs. Additional modules are switched in over the next 50 μs until the full capacitor bank is connected.

Breech and muzzle voltage records for test HPP-3 are shown in Figure 4. The muzzle voltage rises to a peak value of 630 V during fuse vaporization but remains below 500 V as the additional capacitor bank modules are switched on. At peak current of 780 kA, the muzzle voltage is 330 V. The electric field in the plasma is $\sim$ 130 V/cm, a typical value for the high current density in the plasma ($\sim$ 35 kA/cm^2).

The plasma armature is not significantly disturbed by restrike during the test as shown by the sharp rise in muzzle voltage when the projectile leaves the muzzle. This is further confirmed by the rail current probe data shown in Figure 5. The signal from probe #3 shows that the plasma armature has developed a low current tail at 600 μs but there are no separate secondary arcs. The projectile accelerated in test HPP-3 was a Lexan cylinder 23.8 mm ϕ x 19 mm long with a mass of 9 grams. The plasma was initiated with a 0.05 mm thick aluminum foil fuse. The injection velocity was 1.06 km/s. The muzzle velocity, derived from B-dot data and wire switch times, was 3.86 ± 0.05 km/s.

The railgun delivered a momentum change of 25.3 kg·m/s and a kinetic energy increase of 62.1 kJ. Comparing the momentum change to the time integral of $\frac{1}{2}L'$ I^2 yields a mechanical efficiency of 95%. A force loss of 5% is consistent with tests on other high performance railguns at velocities below 4 km/s [5]. The energy efficiency, defined as projectile kinetic energy divided by electrical energy into the breech during the launch time, is 22.8%. The principle electrical losses are stored magnetic energy, 28.7%, and armature dissipation, 31.0%. The balance of the energy loss (17.5%) is due to rail resistance and drag force on the projectile and plasma. The overall efficiency, stored energy to kinetic energy, is only 6.7% due to inefficient matching of the capacitor bank to the railgun.

Physical damage to the railgun bore was observed on all of the high current tests. On Test HPP-3 the rail surfaces were marked by shallow arc tracks (< 0.02 mm deep) over most of the length. Heavier damage occurred in the region traversed by the projectile during the current rise. The heavier damage decreased gradually as the projectile velocity increased to > 2.5 km/s. Damage to the Lexan insulator material included a uniform erosion of 0.02-0.04 mm plus 6 to 8 localized gouges with typical dimensions of 5-8 mm and depth of 0.35-0.4 mm. These gouges are seen on all tests with pressures in excess of 10^8 Pa. The gouges seem to occur primarily in regions where the projectile velocity is less than 2.5 km/s. No gouging was observed at velocities greater than 3 km/s even with a pressure greater than 2x10^8 Pa. The peak pressure on test HPP-3 was 2x10^8 Pa. The pressure on the projectile when it left the muzzle was 9.2x10^7 Pa, near the maximum pressure release that a Lexan projectile can survive without shattering. Projectile integrity was verified by a clean impact hole in a 6.3 mm aluminum plate located 2.2 m from the muzzle.

Rail displacement for all of the HPP tests was very small (< 0.03 mm) due to the high stiffness of the ceramic insulators. Substantially larger displacement were measured for the P and IP tests using G-10 supporting structure. The measured rail displacement for test P-3 is shown in Figure 6. The dashed curve is the effective pressure acting on the inside surface of the rail. The high pressure from 130 μs to 200 μs is caused by the plasma pressure while the remainder of the trace represents the magnetic repulsion force on the rail. The measured displacement has several characteristics that are seen on most tests. The initial negative displacement is a deflection of the rail toward the bore caused by 3-D bending forces. This negative displacement disappears at velocities above 3 km/s when the projectile velocity exceeds the propagation velocity of waves in the railgun structure. The

following positive displacement consists of a nearly harmonic signal at the natural frequency of the rail-insulator system modulated by high frequency signals created by acoustic reflections from the internal structure. Both the amplitude and fundamental frequency are in good agreement with the predictions of a 2-D finite element analysis of the structure.

PLASMA INITIATION SYSTEM

The basis of the plasma initiation system is a short auxiliary railgun located between the injector and the main railgun as shown in Figure 7. The plasma initiator rails are electrically isolated from the railgun rails by a 28 cm long G-10 insulating tube. By employing this isolation, large voltages can be applied to the ionizer rails without causing a breakdown in the main railgun.

Because the ionizer operates in a high pressure gas environment, it is difficult to trigger a discharge across the 18 mm gap between rails. To solve this problem each ionizer rail has an extension built into the insulator as shown in Figure 8. These extensions extend past the center line of the insulator so that ionization from a small trigger discharge is swept across the gap between the extensions by the flowing injector gas. The trigger spark is supplied by a Maxwell Laboratories Model 30103 high voltage trigger generator that provides a 35 kV, 500 ns pulse with an energy of ~ 1 Joule.

The electrical circuit for the ionizer is shown in Figure 9. The sequence of operation is as follows: Passage of the projectile is sensed by pressure switch #1 upstream of the ionizer. After a delay sufficient for the projectile to pass the trigger pin (~ 50 μs), the 35 kV pulser is fired to generate a spark. A further delay of 10 μs allows time for the spark plasma to reach the gap between the rail extensions. At this time, the ionizer bank is discharged, generating a 20 kA current pulse with a width of ~ 200 μs. This discharge starts between the rail extension but is rapidly swept down stream by the injector gas flow. The ionizer discharge is extinguished in about 100 μs as the discharge is swept off of the ionizer rails as shown by the current and voltage waveforms of Figure 10. During the ionizer discharge, ~ 1.7 kJ is dissipated in the plasma. Examination of the ionizer assembly shows arc tracks extending from the rail extensions to the downstream end of the ionizer rails. There is no evidence of arc damage on the G-10 insulation suggesting that the ionizer discharge occurs primarily in the injector gas.

The typical injector gas pressure in the ionizer is 8.3 MPa. At this pressure the 35 kV trigger pulse will not reliably break down the 4 mm surface between the trigger pin and the adjacent electrode. Triggering reliability was obtained by coating the surface between the trigger pin and the rail extension with a thin layer of graphite (Aquadag) before each test. This provided a resistive path (~ 5 kΩ) which flashed independent of gas pressure. Future designs could eliminate the need for this coating by replacing the G-10 surface around the trigger pin with a high resistance carbon insert.

The plasma created by the ionizer discharge flows behind the projectile ~ 28 cm into the railgun rails. During this period of motion (~ ?80 μs), the plasma resistance increases from a few milliohms to ~ 50 Ω as the plasma cools and ions and electrons recombine. When this high resistance plasma enters the railgun rails it draws a small current (~ 10 A) from the dc-bias supply and produces the drop in rail voltage seen in the muzzle voltage trace of Figure 10.

If the full capacitor bank current is switched into the high resistance plasma, a large voltage is developed for a few microseconds until the plasma is reheated. In order to reduce this voltage pulse, only one module is discharged, providing a rising current with dI/dt ~ 600 A/μs. The voltage rises to ~ 1.2 kV for 15-20 μs and then falls to less than 500 V. At this point, the plasma resistance is low enough that the full capacitor bank can be switched on with less than a 50 V increase in plasma voltage. The energy input to the plasma during the reheating phase is ~ 100 J.

A total of 11 railgun tests were performed using the plasma initiator system. A plasma armature was formed reliably on each test.

The highest current prototype railgun test was test IP-21 using the ionizer prototype. On this test (970 kA peak current, 306 MPa), the railgun bore integrity failed in the region of peak current. Plasma was forced into gaps between rail and insulator and behind the Lexan bore liner. The result was an aggravated restrike as seen on the traces in Figure 11. The three tests shown in Figure 11 illustrate the transition from an ideal plasma armature (Test IP-16), where the armature remains short for the entire length of the barrel, to an extended plasma armature (IP-20), where probe signals #5 and #6 show a long tail on the armature near the muzzle, and finally a severe restrike (IP-21), where ~ 10-15% of the input current is flowing in the region between probes 2 and 3 for the entire acceleration time.

CONCLUSIONS

Three prototype railguns were built and tested to verify the railgun mechanical and electrical design for a proposed hypervelocity launcher facility. Measurements of mechanical motion agreed well with 2-D numerical simulations of the railgun response to plasma and magnetic pressure. At the design operating current of 970 kA and an injection velocity of 1 km/s, gaps were opened in the internal structure resulting in an internal failure. This failure mode was expected at an injection velocity of 1 km/s but not at the design injection velocity of 6 km/s. Physical damage in the form of erosion and gouging was observed at velocities < 2.5 km/s with much less damage at higher velocity.

A plasma initiator system was designed to eliminate the erratic behavior exhibited by metal fuse initiators at high velocity and gas pressure. The initiator was successfully tested up to a pressure of 8 MPa using gunpowder propellant. Further tests at higher pressure (40 MPa) in hydrogen gas are needed to qualify this design for operation in a hybrid gas-gun/railgun device.

REFERENCES

[1] W. M. Parson, J. R. Sims, and J. V. Parker, "The Lethality Test System,"
     IEEE Trans. on Magnetics, MAG-22, No. 6, pp. 1641-1644, November 1988.

[2] J. V. Parker, W. M. Parsons, C. E. Cummings, and W. E. Fox, "Performance
     Loss Due to Wall Ablation in Plasma Armature Railguns," AIAA-85-1575,
     presented at AIAA 18th Fluid Dynamics, Plasma Dynamics, and Lasers
     Conference, July 16-18, 1985, Cincinnati, Ohio.

[3] J. R. Asay et al., "Starfire: Hypervelocity Railgun Development for
     High-Pressure Research," IEEE Trans. on Magnetics, MAG-25, No. 1, pp.
     223-227, January 1989.

[4] R. F. Davidson, W. A. Cook, D. A. Rabern, and N. M. Schnurr, "Predicting
     Bore Deformation and Launcher Stresses in Railguns," IEEE Trans. on
     Magnetics, MAG-22, No. 6, pp. 1435-1440, November 1986.

[5] R. S. Hawke, W. J. Nellis, G. H. Newman, J. Rego, and A. R. Suseoeff,
     "Summary of Launcher Experiments Performed at LLNL," IEEE Trans. on
     Magnetics, MAG-22, No. 6, pp. 1510-1515, November 1986.

TABLE I

SHOT #	PROJ MASS (g)	INJECTION VELOCITY (km/s)	PEAK CURRENT (kA)	MUZZLE VELOCITY (km/s)	COMMENTS
P-1	9.0	1.06	438	2 60	
P-2	9.0	1.16	560	3.16	muzzle arc - 8% I_{max}
P-3	9.0	1.08	673	3.75	weak muzzle arc
P-7	8.9	1.08	750	4.03	strong muzzle arc - 30% I_{max}
P-8	9.0	0	930	4.0	restrike arc
HPP-3	9.0	1.06	780	3.86	
HPP-4	9.0	1.07	880	4.15	
HPP-6	15.1	0.99	777	2.89	3.5 g steel sphere in sabot
IP-18	3.5	1.08	200	1.79	
IP-19	8.5	1.07	400	2.74	
IP-20	8.5	1.05	690	3.76	
IP-21	8.5	1.06	940	4.84	weak precursor arc

PHOTONIC
SENSOR

ARMATURE
B-DOT/PHOTONIC
SENSOR

RAIL
B-DOT

CORE MATERIALS
◻ COPPER
▨ POLYCARBONATE
▥ G-10 LAMINATE

STEEL
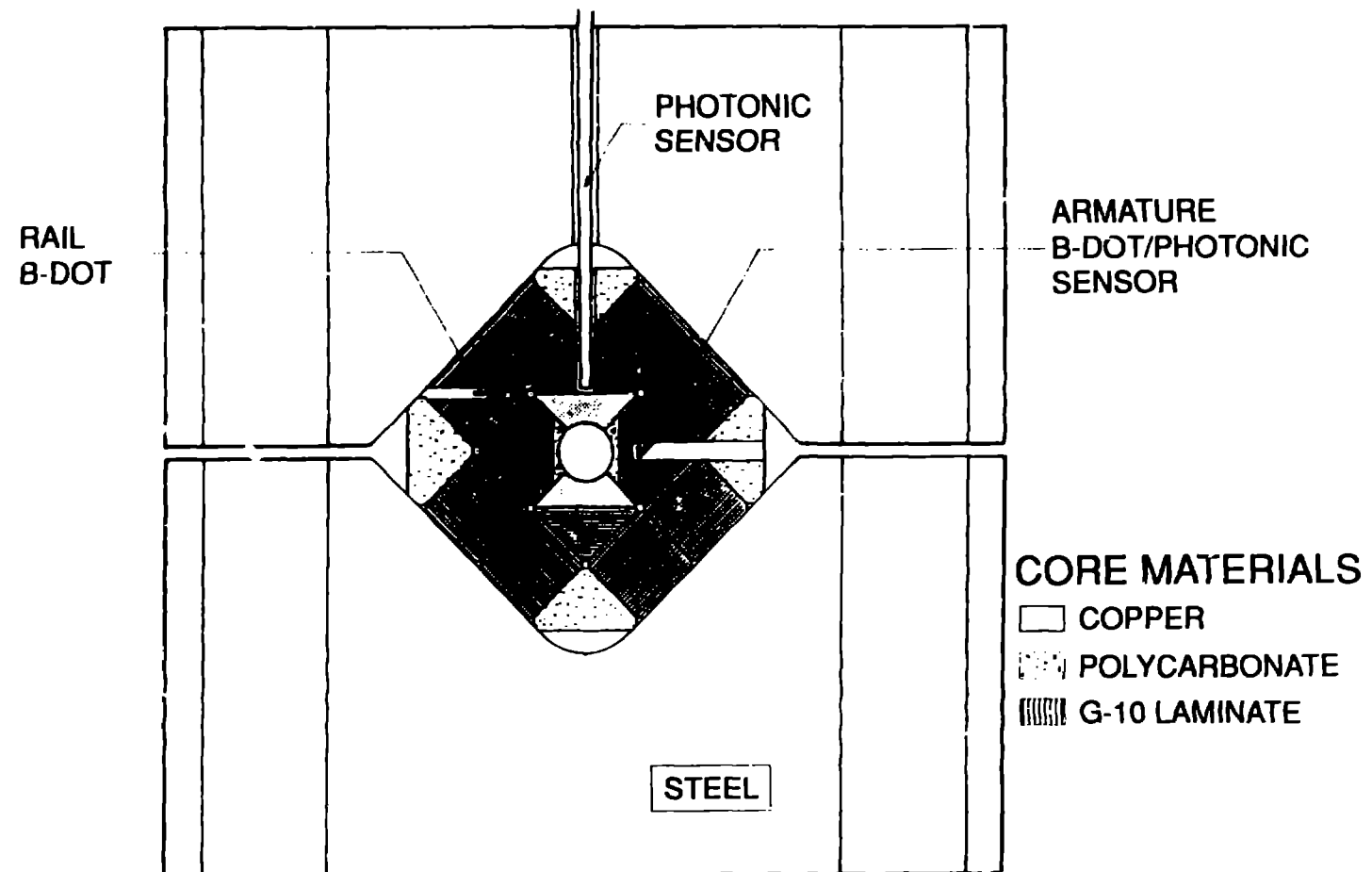
Figure 1. Cross section of LTS railgun.
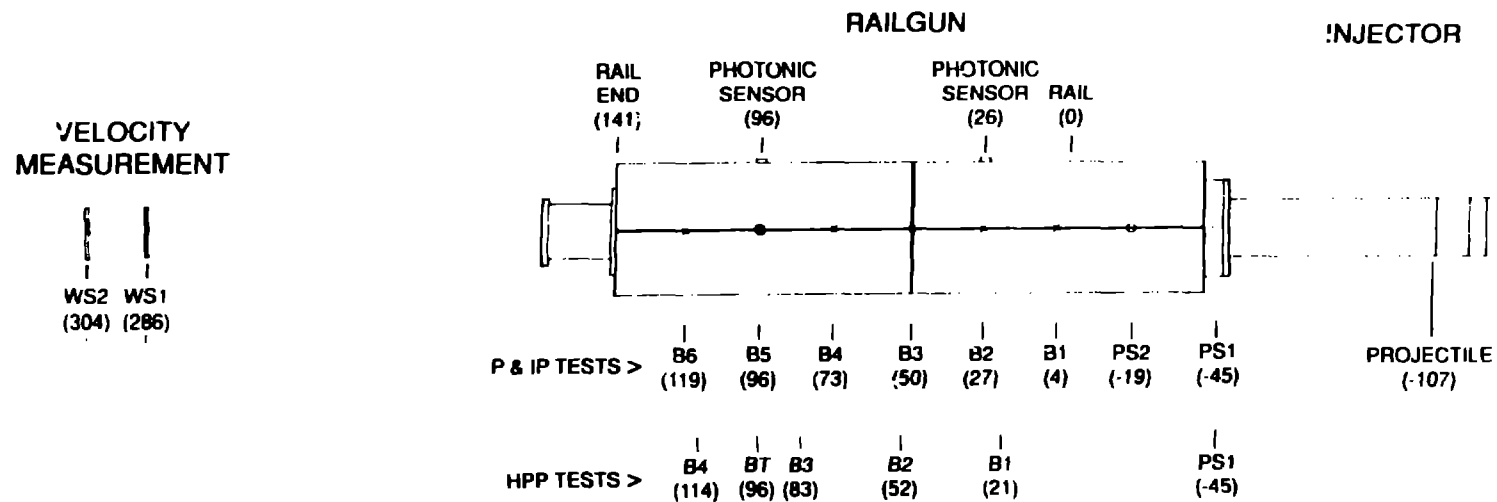
Figure 2.   Layout of prototype railgun.   Position of diagnostics in centimeters
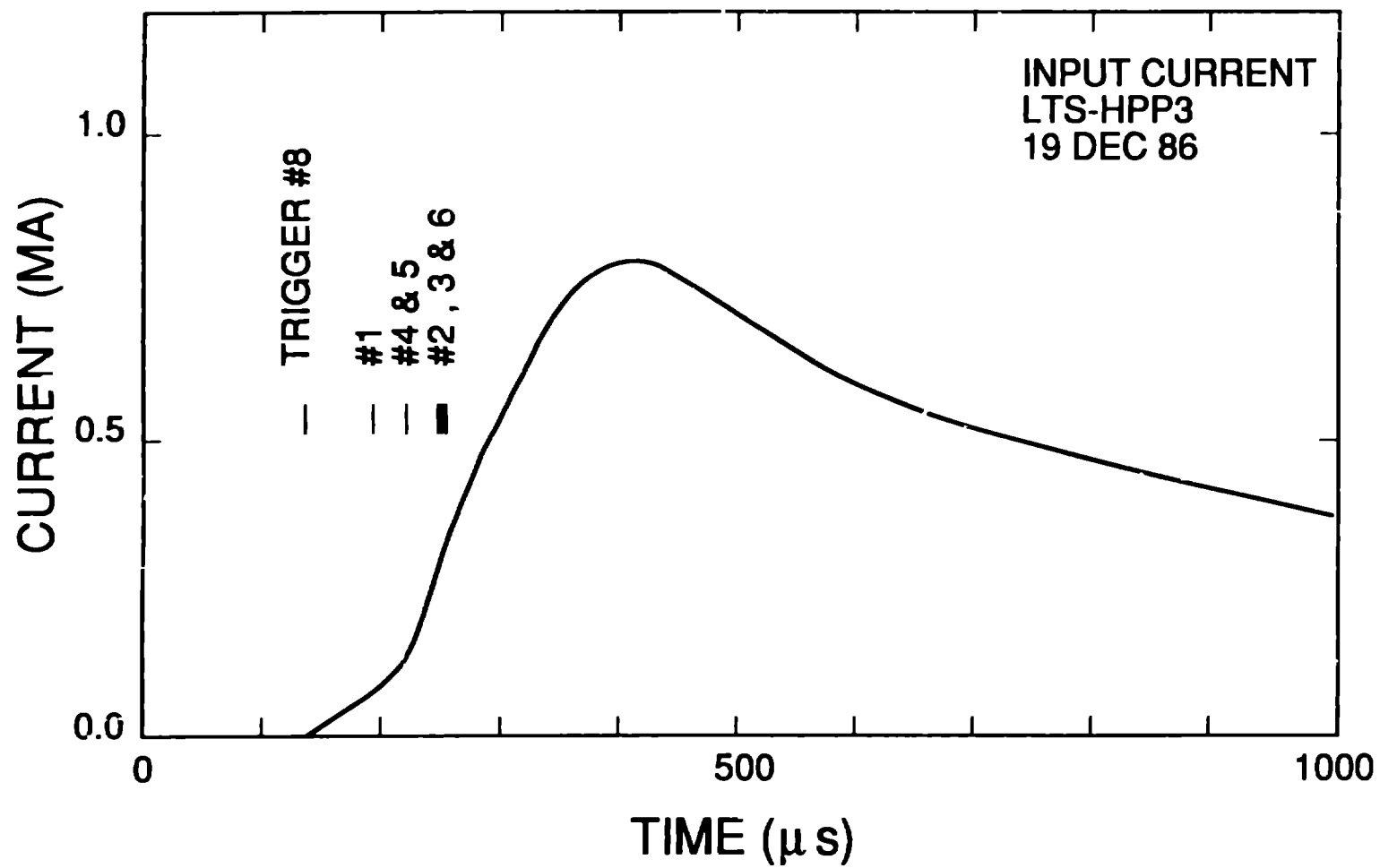shown in parenthesis.
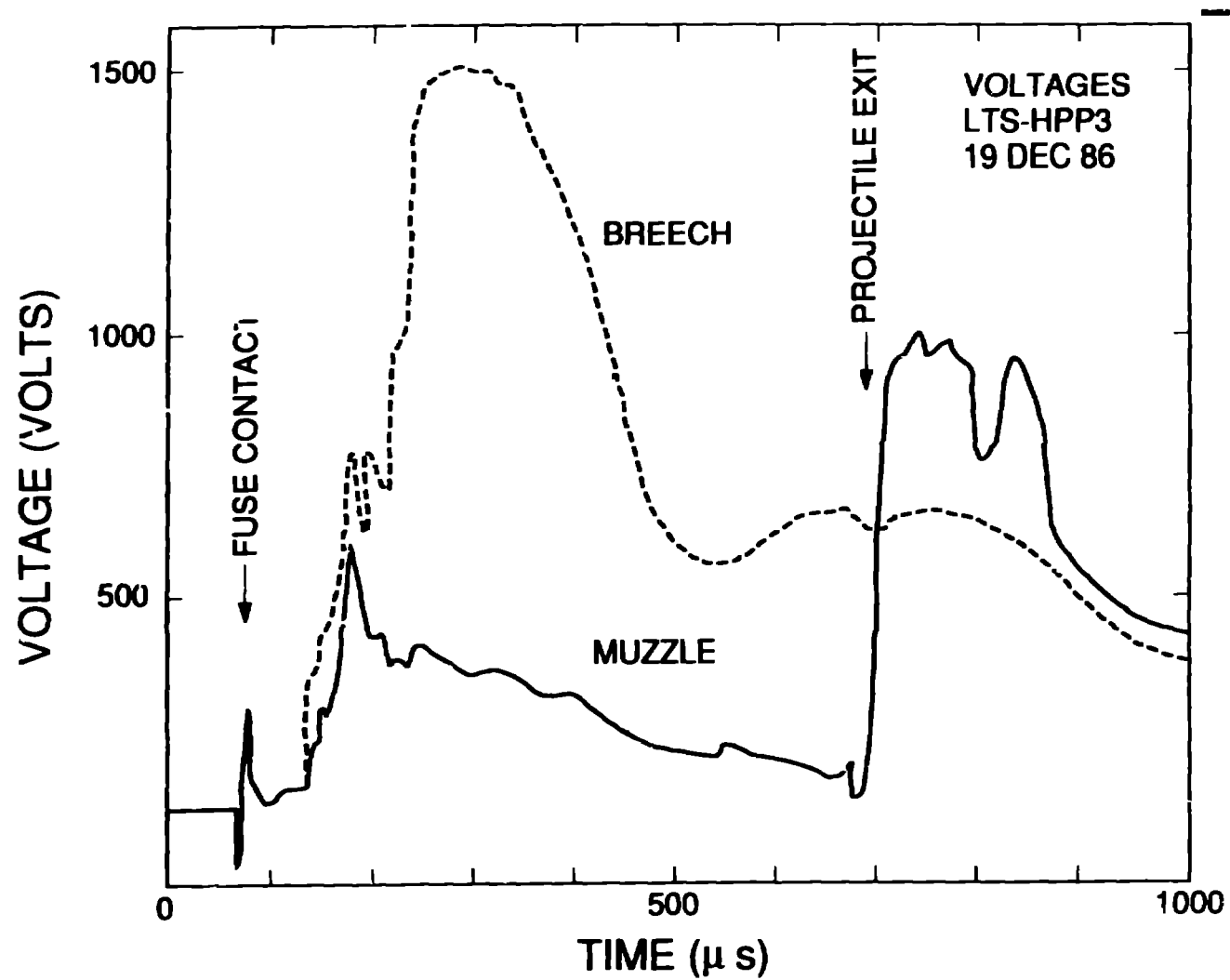
Figure 3. Current waveform for test HPP-3.

Figure 4. Breach and muzzle voltage waveforms for prototype test HPP-3.
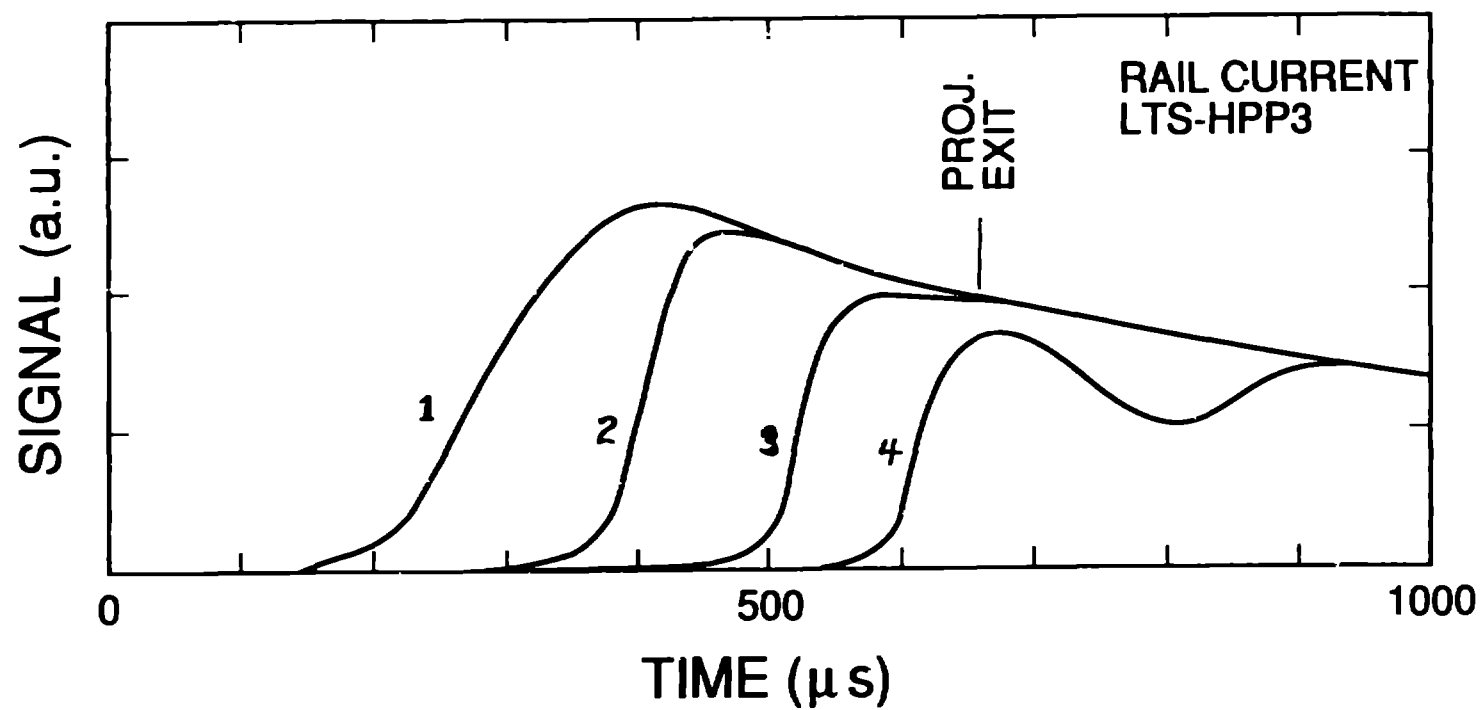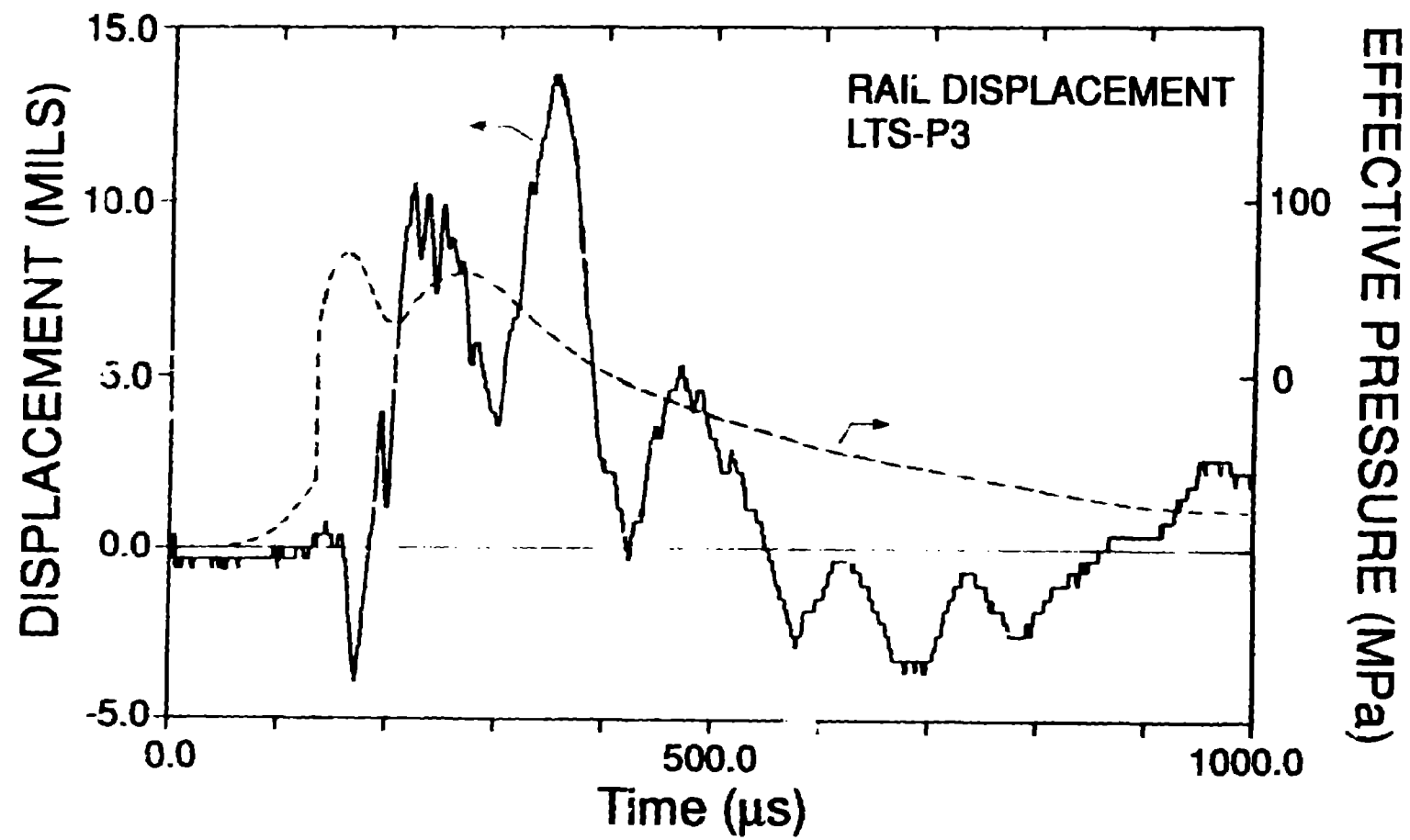
Figure 5. Rail current probe signals for test HPP-3.

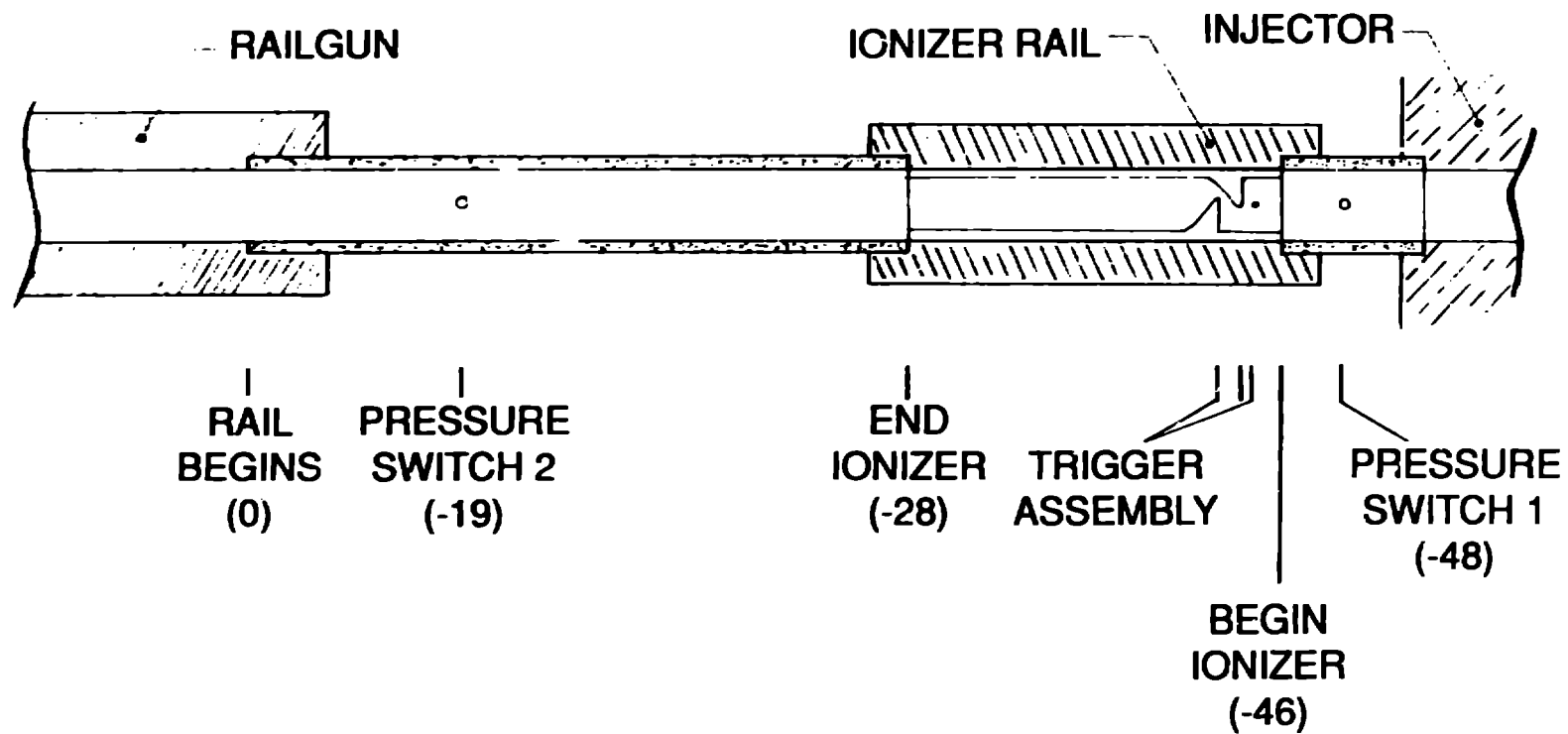Figure 6. Measured rail displacement for prototype test P-3 and the effective driving pressure.

RAILGUN **IONIZER RAIL** **INJECTOR**

| | | | |
RAIL | PRESSURE | END | | PRESSURE
BEGINS | SWITCH 2 | IONIZER | TRIGGER | SWITCH 1
(0) | (-19) | (-28) | ASSEMBLY | (-48)

BEGIN
IONIZER
(-46)

Figure 7.   Schematic layout of the plasma initiator used to eliminate
metallic fusing for the IP tests.

UPPER RAIL
EXTENSION

TRIGGER
PIN

COPPER
RAIL

1 cm

LOWER RAIL
EXTENSION

RESISTIVE
FILM

G-10
LAMINATE
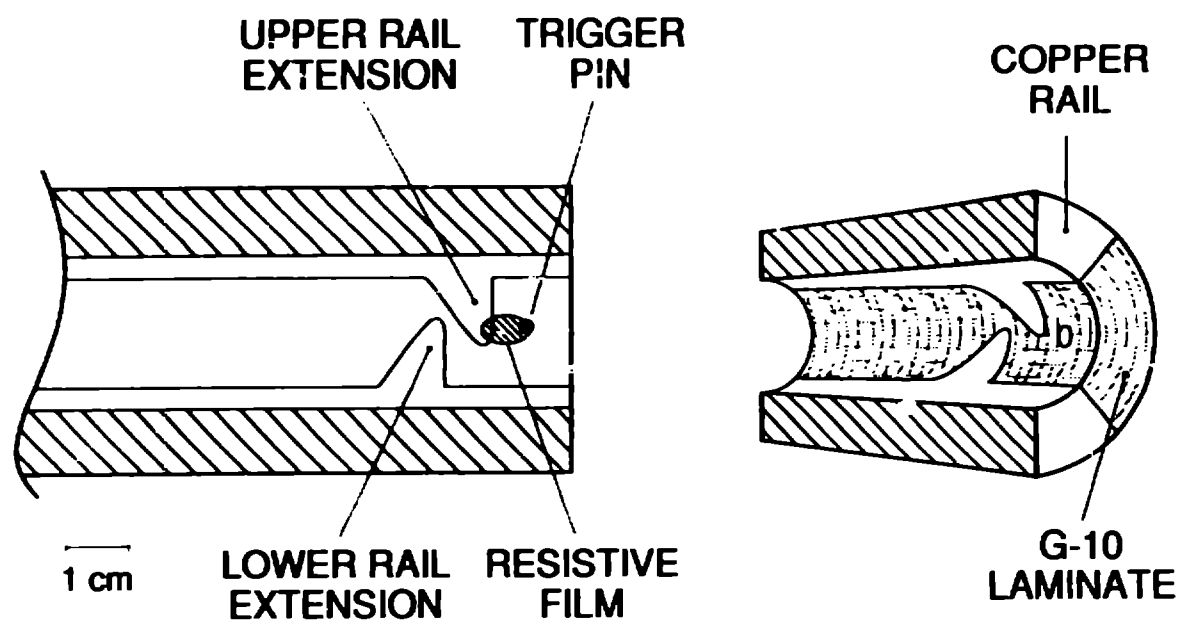
Figure 8.   Details of the trigger electrodes for the plasma
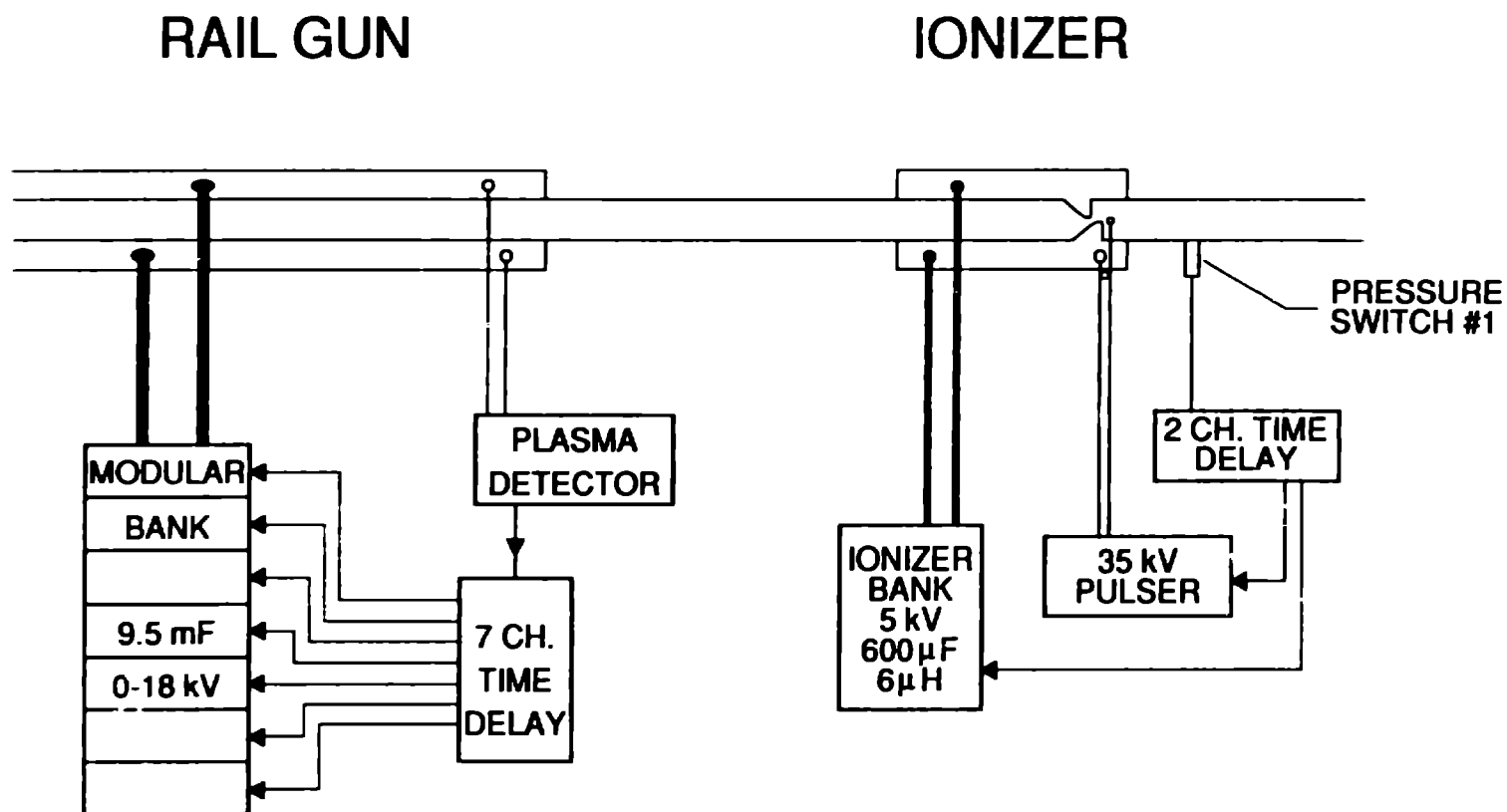   initiator.

Figure 9.   Circuit schematic for the plasma initiator
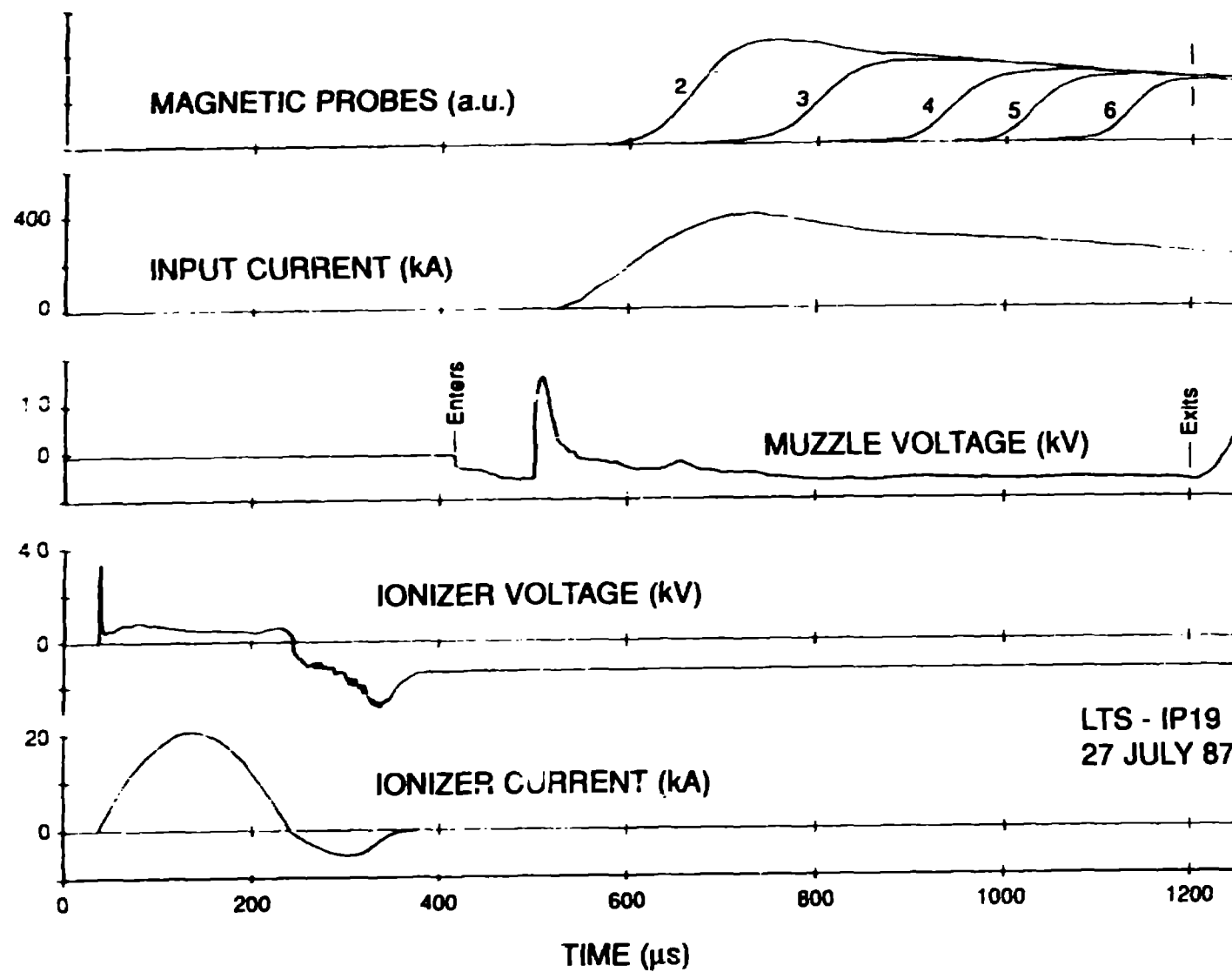and prototype railgun for the IP tests.

Figure 10. Waveforms for test IP-19 showing ionizer operation and timing of plasma entry into railgun bore.
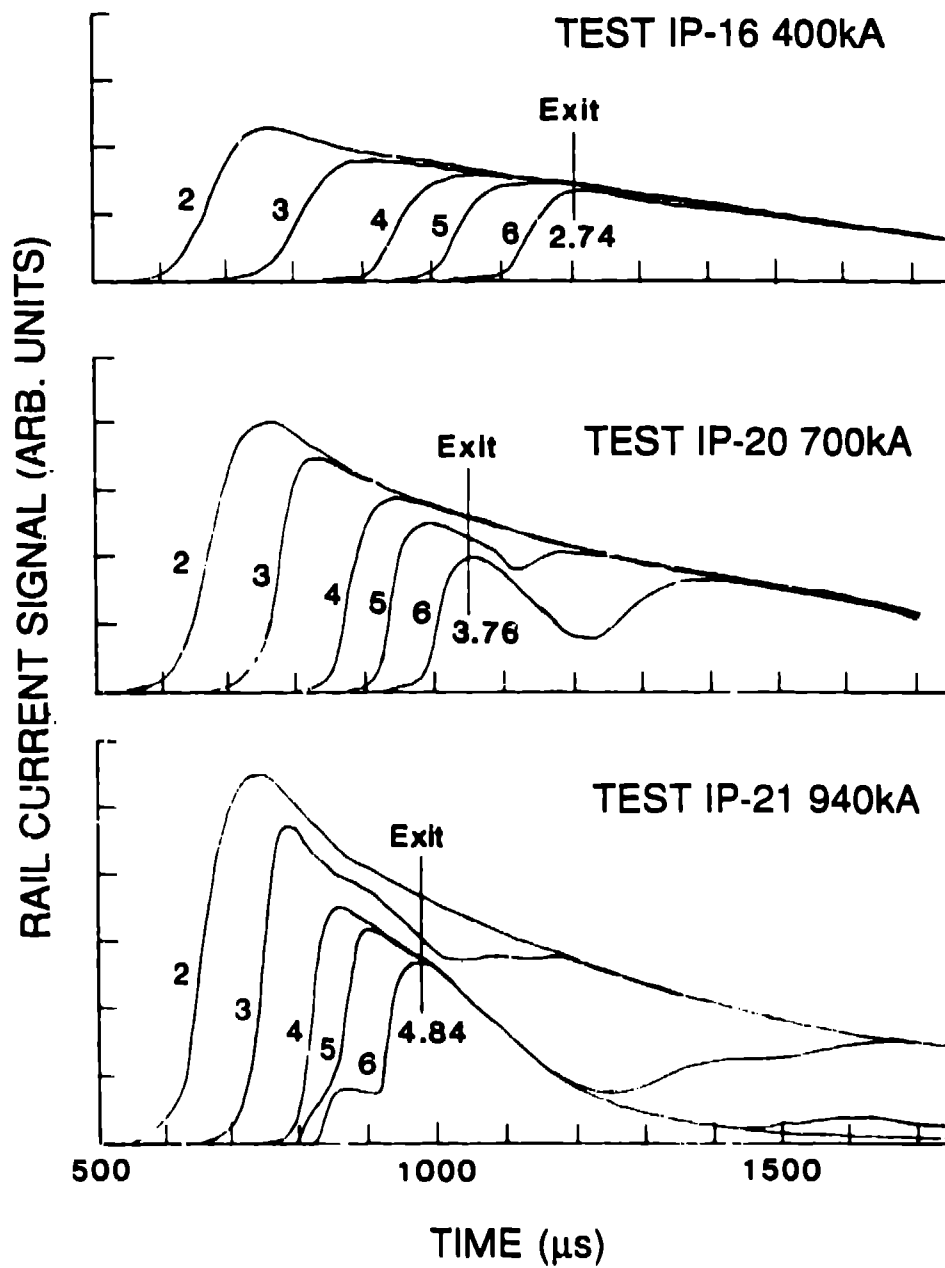
Figure 11. Comparison of rail current signals for three IP tests showing onset of restrike arc formation with increasing velocity.